EES Solar

PAPER

View Article Online
View Journal

Cite this: DOI: 10.1039/d6el00014b

Green solvent engineering for sustainable recovery and circular use of perovskite solar cells

Yash Taneja[ab] and Ranbir Singh *[ab]

Perovskite solar cells (PSCs) offer a transformative path for harvesting renewable solar energy, yet their long-term sustainability relies upon addressing lead toxicity through circular economy principles, with recycling as a key strategy to overcome environmental hazards and recover valuable materials. This approach shows a critical pathway for mitigating hazardous contamination while reclaiming valuable materials. In this paper, a high-efficiency recycling procedure has been proposed on degraded PSCs with the help of a layer-by-layer solvent extraction procedure, with the assistance of green solvents like ethyl acetate (EA) and dimethyl sulfoxide (DMSO). EA and DMSO were selected based on their complementary roles in the recovery strategy for PSCs. EA facilitates dual recovery by selective extraction and phase separation, while DMSO, being a well-established solvent for perovskite precursor synthesis, enhances dissolution and enables efficient material recovery. This approach enables the systematic recovery of the gold (Au) electrode, spiro-OMeTAD layer, perovskite, and indium tin oxide (ITO) coated glass substrate. The quality of the recovered materials is verified by using a combination of X-ray diffraction (XRD), UV-visible spectroscopy, and scanning electron microscopy (SEM), and it was observed that their morphological and photophysical properties are preserved after recycling. Moreover, PSCs fabricated using these recycled components achieved a power conversion efficiency (PCE) of 16.03%, which is a retention of over 90% of the performance of the fresh device with a material recovery rate exceeding 95%. This study creates a commercially feasible, environment-friendly framework of PSC recycling and assists in significantly mitigating the environmental impact of lead-based photovoltaics.

Received 2nd February 2026
Accepted 3rd April 2026

DOI: 10.1039/d6el00014b

rsc.li/EESSolar

Broader context

This study introduces an eco-friendly recycling method for end-of-life PSCs *via* a sequential solvent extraction technique employing benign green solvents. This process recovers over 95% of the materials and refabricated solar cells from recycled materials achieved a PCE of 16.03%, retaining more than 91% of the performance compared to pristine materials. Overall, this research validates the use of green-solvent component recovery as an effective route for recycling PSCs while retaining high device performance.

1. Introduction

Perovskite solar cells (PSCs) have attracted significant research interest due to their exceptional photovoltaic properties, which have led to a remarkable increase in efficiency from 3% to over 27% within a short period.[1] The tuneable band gap, strong absorption, high power conversion efficiency (PCE), and low cost make them highly competitive compared to silicon and other thin film-based photovoltaic technologies.[2,3] PSCs face two major challenges that hinder their widespread adoption.[4] The first is their instability due to prolonged exposure to oxygen, moisture, and high temperatures, leading to rapid material degradation.[5] The second is the presence of elements such as lead (Pb) in PSCs, which poses a significant environmental risk due to potential bioaccumulative toxicity.[6–8] These devices unavoidably accumulate large amounts of waste, which can cause serious environmental impacts. Addressing these challenges is imperative to enhance the long-term stability and environmental compatibility of PSC technology.[9,10] Another fundamental limitation in PSC development is the use of expensive and scarce metals like gold (Au) and indium (In), which poses a significant barrier to large-scale commercialization.[11] Economic assessments based on laboratory-scale manufacturing processes indicate that transparent conductive oxides (TCOs), such as indium tin oxide (ITO) and fluorine tin oxide (FTO) coated glass substrates, account for approximately 50 to 60% of the total device cost, underscoring the urgent need for cost-effective strategies to optimize material utilization and improve overall economic viability.[12,13] Effective recovery and reuse of TCO materials are essential not only for conserving

[a]School of Mechanical and Materials Engineering, Indian Institute of Technology Mandi, Kamand, Mandi, Himachal Pradesh, India. E-mail: ranbir@iitmandi.ac.in
[b]Advanced Energy Conversion Laboratory (AECL), Indian Institute of Technology (IIT) Mandi, Mandi, Himachal Pradesh, 175005, India

valuable resources but also for enhancing the economic feasibility and environmental sustainability of PSC technology.[14] As PSCs continue to gain momentum as a next-generation photovoltaic solution, integrating recycling into their life cycle presents a significant opportunity.[15,16] Establishing robust recycling strategies can mitigate potential supply chain disruptions, reduce reliance on scarce metals, and open the way for a circular economy.[17,18] Effective recycling strategies will not only conserve valuable resources but also mitigate potential supply chain disruptions, ensuring the sustainable advancement of PSC technology.[19,20]

Various studies have been done to replace Pb with other alternatives, but Pb-free PSCs do not exhibit a comparable PCE because of the indirect band gap, increased recombination rates, and poor defect tolerance.[21–23] An early attempt to recover Pb in PSCs was carried out by Park *et al.*, in which an adsorbent was prepared by introducing iron into hydroxyapatite to allow the recovery of Pb in dimethyl formamide (DMF) and nitric acid (HNO_3) solutions.[24] The Larini group reported a green method to recover the electron transport layer (ETL) coated TCO by using dimethyl sulfoxide (DMSO).[25] The recovered ITO/tin oxide (SnO_2) substrate was used to prepare new devices, with the champion efficiency reported to be similar to that of the freshly fabricated devices. Gunasekara *et al.* used a water-based recycling process to recover FTO/SnO_2 substrates.[26] Kim *et al.* successfully recovered Au, and ETL coated TCO glass substrates using polar aprotic solvents such as DMF and γ-butyrolactone (γ-GBL).[27] Similarly, Kadro *et al.* developed a multistep process combining chlorobenzene and ethanol to reclaim glass substrates while preserving the TiO_2 layer.[28] Feng *et al.* reported a recycling method to recover each material in the perovskite by closing loop recycling using butylamine, toluene, and ethanol solution to recover silver electrodes, ITO substrates, and perovskite crystals, respectively.[29,30] While research has shown that PSC materials can be selectively dissolved and separated, current methods heavily rely on toxic solvents like DMF, chlorobenzene, and γ-GBL, raising serious environmental and safety concerns.[31,32] The problem with these methods is that they either recover only one material or use another harmful substance to do the recycling, which defeats the purpose since a toxic material is being used to recover another toxic material.

In our study, we have introduced green solvents to recover more than 95% of materials from end-of-life PSCs. Solvents such as ethyl acetate (EA) and DMSO are used to recover and recycle degraded PSCs. The research is mainly focused on recovering every material used in a planar glass/ITO/SnO_2/methyl ammonium formamidinium lead iodide ($MAFAPbI_3$)/Spiro-OMeTAD/Au-based PSC by applying a layer-by-layer solvent extraction approach with the help of green solvents. The recycling process successfully recovered key components such as the perovskite powder, spiro-OMeTAD, Au electrode, and glass/ITO substrate. The purity of the recovered materials was confirmed through UV-visible absorption spectroscopy and X-ray diffraction (XRD) analysis, which showed that glass/ITO substrates, recycled perovskite powder, spiro-OMeTAD, and Au were sufficiently pure for direct reuse in PSCs. Also, the recovered materials were used to fabricate a fresh set of PSCs, and a PCE of 16.03% was achieved, which is over 90% that of the reference PSC that was fabricated using the fresh material.

2. Experimental section

2.1. Materials used

Ethyl acetate (EA, 99.5%, extra pure), anhydrous DMSO (99.9%), and hydrochloric acid (HCl, 37.7%) were purchased from Loba Chemie and were used for the recovery of spiro-OMeTAD, Au, perovskite, and glass/ITO. The materials required for device fabrication, like SnO_2 (99.9%), methyl ammonium (MAI), formamidinium iodide (FAI), lead iodide (PbI_2), DMSO, DMF, toluene, and chlorobenzene, were purchased from Sigma Aldrich. 2,2′,7,7′-tetrakis [*N*,*N*-di(4-methoxyphenyl)amino]-9,9′-spirobifluorene (spiro-OMeTAD), bis(trifluoromethane) sulfonimide lithium salt (Li-TFSI), tris(2-(1*H*-pyrazol-1-yl)-4-*tert*-butylpyridine) (TBP), and cobalt(III) tris (bis (trifluoromethyl sulfonyl) imide) (FK209) were purchased from Tokyo Chemical Industry (TCI) Co., Ltd (Japan). The recovered materials that were used in device preparation were perovskite powder, spiro-OMeTAD, and ITO/glass substrates.

2.2. Thin film characterisation

We obtained UV-visible absorption spectra for the spin-coated films using a UV-visible spectrophotometer (Analytical Technologies Ltd, India). X-Ray diffraction for the thin films was performed using a copper X-ray source (Rigaku, Smartlab, Japan). Photoluminescence (PL) measurement of the perovskite thin film was done using a PL spectrophotometer (Horiba, HR Evolution Japan). A field emission scanning electron microscopy (FE-SEM) image was obtained using a Nova Nano SEM 450 from Thermo Fisher and was used for the morphological analysis of the surface of the recycled perovskite thin film.

2.3. Electrical characterisation

The electrical characterization studies were done using a Fytronix-9712 source meter under one-sun conditions (AM 1.5 G, 100 mW cm^{-2}) using a TriSOL standard solar simulator with a device area of 0.05 cm^2. The intensity of the solar simulator was calibrated using a standard mono-Si solar cell (SN-1000-TC-K-QZ, VLSI standards S/N 105100602) before every set of measurements, which is certified by VLSI Standards Incorporated. EIS measurements were conducted on an Autolab (MAC90173, Metrohm 302N) electrochemical workstation.

3. Results and discussion

The recycling process was initiated by targeting the selective delamination of the top device layers to isolate the perovskite absorber. Discarded PSCs were completely submerged in an EA bath for a five-minute duration. EA was strategically selected for its dual functionality as it serves as a highly effective solvent for the spiro-OMeTAD HTL while simultaneously disrupting the interfacial adhesion of the Au electrode. This process reduces the mechanical handling by combining Au removal and HTL extraction into a single step without damaging the reclaimable

perovskite layer. EA is employed to facilitate the detachment of the Au electrode and the removal of the spiro-OMeTAD layer due to its favorable interaction with the organic HTL and its ability to weaken the adhesion between spiro-OMeTAD and the metal contact.

The solution containing the dissolved organic constituents and suspended Au particles was subjected to vacuum filtration through Whatman filter paper. This step helps in the collection of Au particles and the separation of EA through simple filtration. Fig. 1a shows the systematic sequence of this recovery procedure. To confirm the chemical composition of the filtrate and to guarantee the successful extraction of the hole transport material, the EA solution was analysed through UV-visible spectrophotometry (Fig. 1b). The absorption spectrum that was obtained had a clear peak typical of spiro-OMeTAD, giving conclusive evidence that only the HTL was dissolved in the solvent and the perovskite layer remained intact. To further assess the chemical stability of the recycled material, FTIR spectra of both fresh and recycled Spiro-OMeTAD were compared, as shown in Fig. S1. The superimposition of the spectral peaks demonstrates that no new functional groups were introduced and no existing bonds were cleaved. This indicates that the recycling protocol successfully recovers the Spiro-OMeTAD while retaining its structure and chemical purity. This spectroscopic study proves the effectiveness of EA as a selective stripping agent, which guarantees the successful extraction of the organic and metallic materials of the perovskite absorber.[33] Simultaneously, XRD of the filtered solid residues was used to verify the purity of the recovered Au. Fig. 1c depicts that the XRD pattern has characteristic peaks of 38.2°, 44.4°, 64.6°, and 77.5° corresponding to (111), (200), (220), and (311) planes, respectively.[34] These findings confirm that filtration was effective in isolating the metal without any impurities and unreacted precursors being left behind by the process.[35]

The second phase of the reclamation process focused on the selective dissolution of the perovskite absorber. Substrates were immersed in a bath of pure anhydrous DMSO (Fig. 2a), a solvent chosen for its high dielectric constant and ability to form a stable coordination complex with PbI_2 *via* the oxygen atom in the sulfonyl group (S=O). Upon immersion, the perovskite film rapidly transformed into the liquid as the dissolution reached completion in less than 60 seconds. This procedure was useful to remove the absorber layer, leaving the SnO_2 (ETL) on the ITO-coated glass. High solubility of the MA/FA cations and lead halides in the polar aprotic DMSO solvent is responsible for the fast dissolution of the perovskite layer.

The DMSO solution containing dissolved perovskite was slowly introduced to hot chlorobenzene to crystallize the perovskite material. Chlorobenzene is used in this configuration as a non-polar antisolvent that significantly reduces the solubility level of the perovskite precursors. High miscibility between DMSO and chlorobenzene supports the rapid diffusion of DMSO in the chlorobenzene phase, leading to the nucleation of perovskite nanocrystals. This approach mirrors the solvent-engineering approach that has been used in the manufacturing of PSCs. Heated antisolvent is an important control parameter of the phase transition of the recovered perovskite. An increase in chlorobenzene temperature increases the pace of perovskite crystallization. The thermal energy instantly causes supersaturation, which causes the perovskite in the solution to crystallize and precipitate as a black powder in the chlorobenzene.[36,37] The process was repeated 3 times, and the solvent was decanted to obtain the precipitate. The

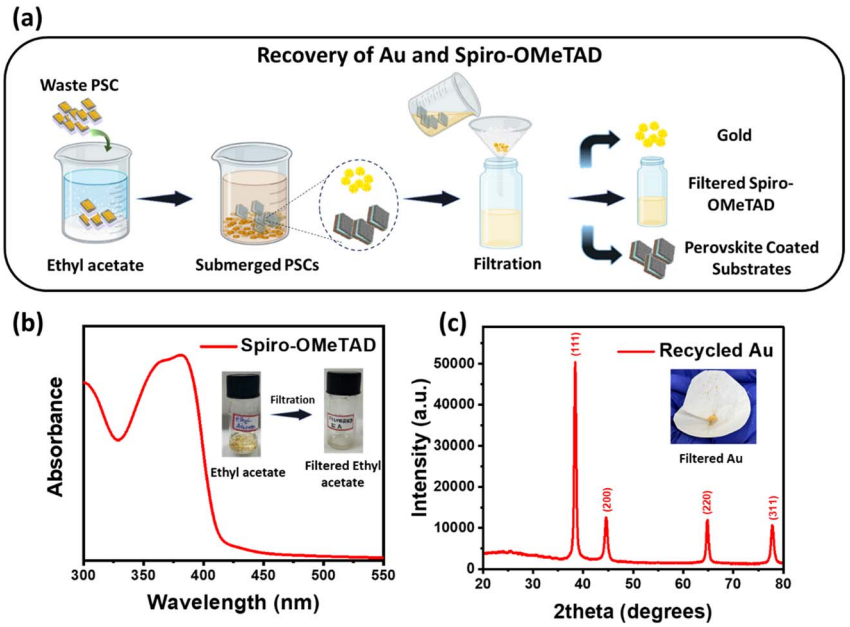

Fig. 1 (a) Schematic showing the recovery of Au and spiro-OMeTAD in the first step. (b) UV-visible data for recovered spiro-OMeTAD (inset image shows a glass vial containing Au particles dispersed in EA, from which the Au is retrieved *via* filtration). (c) XRD plot for Au particles recovered after filtration (inset image shows the collected filtered gold on Whatman filter paper).

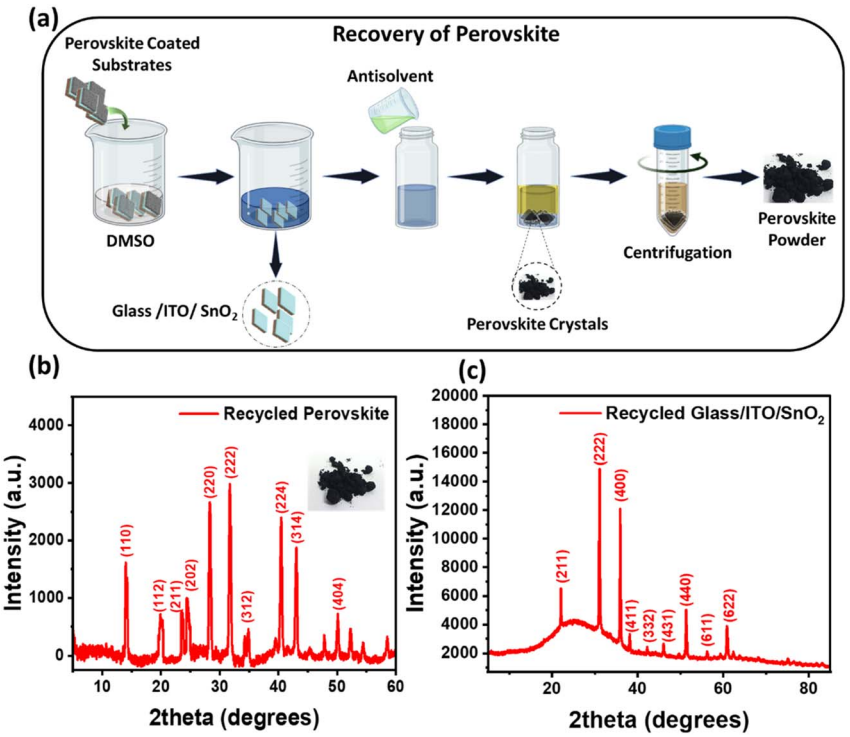

Fig. 2 (a) Recovery of perovskite powder and glass/ITO/SnO_2 substrates *via* solution processing. (b) XRD plot for recovered perovskite powder formed after the addition of antisolvent (inset shows the image of the obtained perovskite powder). (c) XRD data for recovered glass/ITO/SnO_2 substrates.

perovskite powder was then dried in a vacuum oven at 100 °C and stored under N_2 conditions for future use. The XRD analysis done for the perovskite film is shown in Fig. 2b. The principal peaks of $MAFAPbI_3$ at 2θ values of 14.08° (110), 28.5° (220), and 32° (310) confirm the presence of $MAFAPbI_3$ crystals.[38] The XRD analysis of glass/ITO/SnO_2 substrates shown in Fig. 2c revealed that, due to the amorphous nature, the SnO_2 layer did not exhibit distinct diffraction peaks. In contrast, the ITO layer displayed prominent crystalline peaks, dominating any potential signals from the SnO_2.[39]

The final stage of the recycling procedure, as shown in Fig. 3a, focused on the isolation of the ITO-coated glass substrates through the selective removal of the SnO_2 ETL. To achieve this, the substrates were briefly immersed in a diluted HCl solution of 1.7 M concentration. This step relies on the differential chemical stability of the two oxide layers. This concentration was specifically calibrated to achieve complete etching of the SnO_2 without degrading the quality of the underlying ITO layer. Optimization of the HCl concentration and reduction of the exposure time to 30 seconds allowed the removal of the SnO_2 without compromising the chemical integrity of ITO-coated glass substrates. The substrates were immediately dried in an oven at 100 °C after immersion in order to prevent any chemical activity from the residual HCl. The recovered glass/ITO substrates were then tested in terms of crystallinity and quality by XRD analysis. As shown in Fig. 3b, the diffraction patterns of the recycled glass/ITO substrates are identical to those of unused glass/ITO substrates, as shown in Fig. S2. XRD peaks at 21.5° (211), 30.6° (222), and 35.5° (400) and the absence of any extraneous peaks or shifts in the characteristic ITO reflections suggest that the selective etching process successfully removed the SnO_2 while preserving the underlying ITO. UV-visible spectroscopy was also used to further confirm the step-by-step removal of the layers of the device (Fig. 3c). Initial treatment with EA did not show any changes in the perovskite absorption spectrum, which confirms that while EA is effective for electrode and HTL delamination, it is not chemically reactive to the perovskite absorber and thus the film remains physically intact.[40] In contrast, the complete disappearance of the characteristic perovskite absorption upon immersion in DMSO was observed, indicating the overall dissolution of the perovskite layer. The remaining spectrum of the DMSO-treated substrate shows a sharp absorption onset at 350 nm, consistent with bandgap absorption of the underlying SnO_2 and glass/ITO layers.[41] Additionally, to confirm the functional integrity of the recovered substrates, both the electrical and optical properties of the fresh and recycled ITO substrates were evaluated.[42] Sheet resistance measurements *via* the four-probe method showed only a marginal increase from 11 Ω sq^{-1} for the fresh ITO to 12.5 Ω sq^{-1} for the recycled ITO, indicating excellent preservation of electrical conductivity. Furthermore, UV-visible spectroscopy revealed that the transmittance spectrum of the 1.7 M HCl recycled ITO is nearly perfectly superimposed onto that of the fresh ITO across the visible wavelength range, as shown in Fig. S3. The simultaneous retention of low sheet resistance and high optical transparency

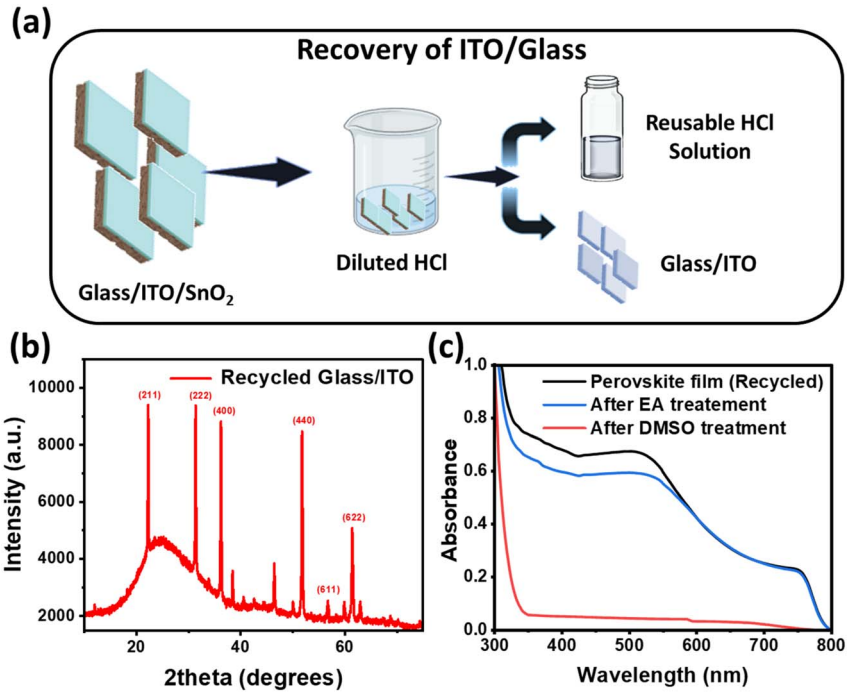

Fig. 3 (a) Steps involved in the recovery of ITO coated glass substrates using a diluted HCl solution. (b) XRD data for recovered glass/ITO substrates and (c) UV-visible spectroscopy plots of recycled perovskite films and substrates obtained after treatment with EA and DMSO.

confirms that the recycled ITO remains suitable for refabricating PSCs. The surface morphology of the fresh and recycled ITO substrates was also examined using SEM, as shown in Fig. S4. The fresh ITO exhibits a uniform and compact granular morphology characteristic of ITO films. In contrast, the recycled ITO surface appears relatively smoother with less pronounced grain features. This change in surface appearance is likely associated with the chemical treatment during the recovery process, which can partially modify the topmost surface of the ITO layer.

Following the recovery process, the recycled material was reused to fabricate new PSCs using the fabrication protocol outlined in the SI with the device structure illustrated in Fig. 4a. The FE-SEM images in Fig. 4b and c show that the recycled film has smaller grains than the reference film. Also, cross-sectional SEM images shown in Fig. S5 demonstrate that the complete device architecture is successfully reproduced on the recycled substrate, displaying well-defined interfaces and dense perovskite morphology highly comparable to those of the reference film. The slightly reduced thickness observed in the top Spiro-OMeTAD layer of the recycled device is a direct result of the lower solution concentration utilized during its deposition. The XRD spectra of the perovskite film depicted in Fig. 4d show a very small PbI_2 peak at 12.4°, which implies that the process used for the extraction of perovskite is pure and the recycling process is highly efficient.[43,44] The optoelectronic quality of the reclaimed material was evaluated using PL spectroscopy, with the emission profiles of the recycled and reference films compared in Fig. 4e. The peak intensity of the PL spectrum remains comparable to that of the reference, showing only a small reduction. This sustained emission intensity suggests that the film coated using recovered material retains a high quality despite the recycling process.[45]

The viability of the recycling process was examined on the basis of the current density (J_{sc}) *versus* open circuit voltage (V_{oc}) curve presented in Fig. 4f and Table 1 summarizing other electrical parameters of the PSCs. The reference device, which was made using fresh materials, showed a PCE of 17.62% and a V_{oc} of 0.96 V. However, the devices fabricated using the recycled materials showed a remarkable PCE of 16.03% and a V_{oc} of 0.92 V. The conservation of more than 90% of the original efficiency is indicative of the high quality of the recovered materials. The slight decrease in the FF from 73.12% to 71.91% could be attributed to smaller grain sizes in the recycled perovskite films and also to the lower thickness of the HTL, which can cause some resistive losses at the grain boundaries and interface.[46,47] The fabricated PSCs were subjected to various optoelectronic characterization studies to explore the charge recombination kinetics and long-term stability. To determine the degree of bimolecular recombination, J_{sc} and light intensity (I) plots were analyzed, which are dependent on the power law equation, $J_{sc} \propto I^{\alpha}$, where I is light intensity, and α is a power law constant.[48] As shown in the J_{sc} *vs.* I plot (Fig. 4g), the α values for the reference and recycled PSCs were calculated to be 0.99 and 0.98, respectively. The proximity of these values to unity suggests that bimolecular recombination is effectively suppressed in both device types under short-circuit conditions. The corresponding J–V curves for these intensity variations are provided in the SI (Fig. S6). Furthermore, the dependence of the open-circuit voltage on light intensity was evaluated using the

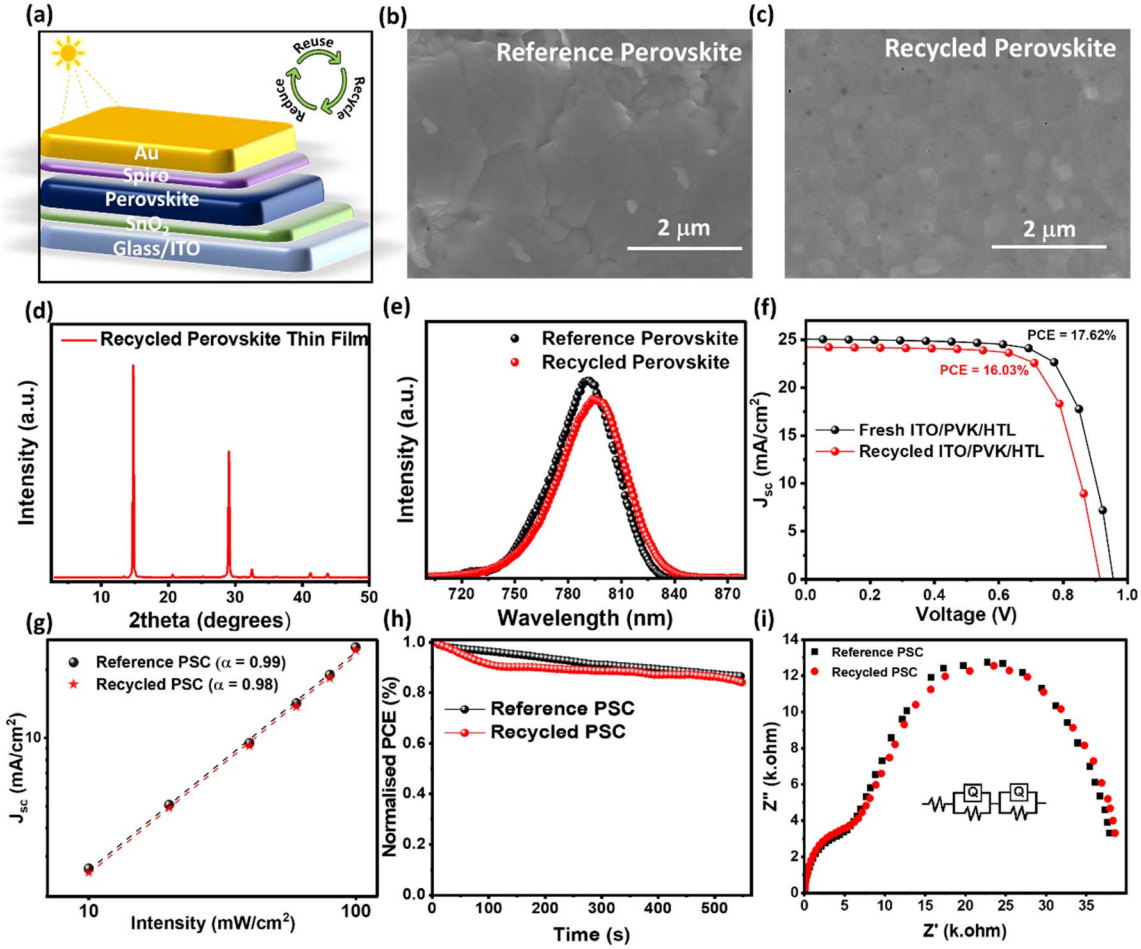

Fig. 4 (a) Device structure showing each layer used in the fabrication of PSCs. (b and c) FE-SEM images of reference perovskite and recycled perovskite thin films. (d) XRD plot of the recycled perovskite thin film. (e) PL plots for the fresh and recycled perovskite films. (f) J_{sc} *vs.* voltage (V) curve of the reference PSCs and the device fabricated from recycled materials. (g) J_{sc} *vs.* intensity (I) curve for reference and recycled PSCs showing the power law constant (α). (h) Light soaking stability data showing normalised PCE *vs.* time (s) for reference and recycled PSCs. (i) Nyquist plot for reference and recycled PSCs under dark conditions with an equivalent circuit shown in the inset.

Table 1 Photovoltaic parameters for recycled and reference devices under one sun illumination

Device	J_{sc} (mA cm^{-2})	V_{oc} (V)	FF (%)	PCE (%)
Fresh ITO/MAFAPbI$_3$/Spiro	25.07	0.961	73.12	17.62 17.57 ± 0.07
Recycled ITO/MAFAPbI$_3$/Spiro	24.24	0.920	71.91	16.03 15.77 ± 0.23

following relationship, $V_{oc} \propto \beta \frac{kT}{q} \ln(I)$, where K, T, q, and β indicate the Boltzmann constant, the temperature in Kelvin, the elementary charge, and the reduced ideality factor, respectively.[49] The V_{oc} *versus* intensity plots in Fig. S7 show β values of 1.24 for the fresh device and 1.32 for the recycled device, indicating a slightly higher degree of trap-assisted recombination in the latter.[50] To demonstrate the immediate operational stability of the recycled devices under continuous illumination and to confirm that the recovered materials can sustain stable power output, the operational stability of the devices was assessed through continuous light-soaking tests. As illustrated in Fig. 4h, the normalized PCE plot of the recycled PSCs showed comparative stability, retaining a very similar performance to that of the reference device. Other electrical characteristics like J_{sc}, V_{oc}, and FF for light soaking stability also show similar results (Fig. S8). EIS was also used to analyze the charge transport and for recombination study. The Nyquist plots for both cells exhibit characteristic semi-circles, which were fitted using an equivalent circuit to extract the series resistance (R_s), recombination resistance (R_{re}), and charge-transfer resistance (R_{ct}). According to the EIS data (Table S1 in the SI), the recycled device showed

Table 2 Comparison of reported layer-extraction recycling strategies for PSCs, including solvents used, recovered materials, and PCEs of devices fabricated using fresh and recycled components

Solvents used	Recovered material	Fresh PSC PCE (%)	Recycled PSC PCE (%)	Reference
Aqua regia and DMF	ITO, Pb, gold, and HTL	—	—	9
Chlorobenzene, adhesive tape, and DMF	FTO and PbI_2	14.60	15.40	52
Chlorobenzene, DMF, and ethanol	FTO, PbI_2, and MAI	16.00	16.70	28
KOH	Pb	8.15	8.49	53
Butyl amine	Perovskite, TCO, and NiO_x	17.90	17.46	29
Water and IPA	SnO_2/ITO	19.85	19.33	26
EA, DMSO, and diluted HCl	ITO, perovskite, spiro (HTL), and gold	17.62	16.03	This work

an increase in the R_s value (21.46 Ω) compared to the reference (8.306 Ω), while the R_{ct} values were 5624 Ω and 4890 Ω, respectively. The slightly elevated resistance values in the recycled cell likely contribute to the minor reduction in the Fill Factor (FF) and J_{sc} observed in the photovoltaic performance. Overall, these collected results highlight the substantial potential of material recovery and reuse without severely compromising device performance. The dark *I–V* characteristic shown in Fig. S9 demonstrates that the recycled PSCs retain a behavior highly comparable to that of the reference PSCs, indicating that the reclaimed Pb does not introduce significant electronic defects. Compared to the reference cell, the recycled PSC shows a slight increase in *J–V* hysteresis (shown in Fig. S10). This moderate gap between scan directions points to a minor increase in non-radiative recombination centers within the recycled film. The calculations demonstrating a material recovery rate exceeding 95% are detailed in Table S2. To ensure accuracy, 10 devices with a substrate area of 1.5 cm^2 were processed during recycling, and the mass of each layer was determined following the methodology described in the earlier study.[30] It is important to note that while the proposed recycling and material recovery stage significantly reduces hazardous waste by utilizing the greener EA and DMSO solvent system, the subsequent refabrication of the devices still relies on conventional solvents such as DMF and chlorobenzene to ensure optimal film quality.

4. Solvent analysis

There are several solvents that have been used for recycling PSCs using the solvent extraction approach. In contrast to earlier studies that employed hazardous and toxic solvents such as DMF, chlorobenzene, and 2-methoxyethanol, the present work utilizes relatively greener and more environment-friendly solvents.[17,28] Table S3 presents a comparative assessment of various green chemistry parameters for the solvents used, reinforcing their suitability for sustainable processing.[51] As shown in Table S3, solvents like DMSO and EA have a relatively better safety profile, as they present high scores in the green category for both human health and aquatic toxicity, which depicts that for these solvents, the risk factor is minimal and they are considered safer options compared to many other solvents. However, solvents used in previous studies, like DMF and 2-methoxyethanol, fall in the red zone because of the well-documented negative impact on human health and the environment. The summary of the previous recycling research is presented in Table 2. Although past reclamation attempts have often involved the use of toxic reagents like DMF and 2-methoxy ethanol or purification procedures like column chromatography, this research emphasizes a more environmentally friendly and less toxic working method. This comparative study and solvent analysis help explain why DMSO and EA were chosen as practical alternatives.

5. Conclusion

This study presents a practical and sustainable approach for the recovery and reuse of materials from degraded PSCs, using only eco-friendly green solvents like EA and DMSO. Using a solvent-selective approach, we efficiently separated critical materials such as perovskite, spiro-OMeTAD, Au electrode, and glass/ITO substrates from non-functional PSCs. UV-visible spectroscopy and XRD analysis confirmed the successful isolation and purity of each recovered material. These recovered materials were subsequently used to refabricate PSCs. The refabricated device delivered a PCE of 17.62% with a V_{oc} of 0.96 V, while the device fabricated from recycled materials achieved a PCE of 16.03%, retaining over 90% of the original efficiency. The slight decrease in the FF was attributed to slight imperfections in the recycled perovskite film. These results confirm that the recovery process does not compromise functionality and validate the potential for fully reusing components from failed devices. By relying solely on green solvents and enabling the recovery of over 95% of materials from non-operational PSCs, this approach significantly reduces environmental impact and material costs. It eliminates the dependence on expensive raw materials and offers a cost-effective, low-waste route for future photovoltaic technology. Overall, this approach promotes circular material usage and opens up new opportunities for scalable, sustainable, and economically viable PSC manufacturing.

Conflicts of interest

The authors state that there are no conflicts of interest.

Data availability

The data that support the findings of this study are available from the corresponding author upon reasonable request.

Supplementary information (SI): the device fabrication processes along with various physical, electrical, and morphological information regarding the recovered and fresh material. See DOI: https://doi.org/10.1039/d6el00014b.

Acknowledgements

R. S. acknowledges the Core Research Grant (grant no. CRG/2022/003088), SERB project, and Indian Institute of Technology Mandi, India, for providing the experimental facilities in the Advanced Material Research Centre (AMRC) and Centre of Design and Fabrication of Electronic Devices (C4DFED).

References

1 M. Osman, *et al.*, Enhanced performance of perovskite solar cell *via* up-conversion YLiF4: Yb, Er nanoparticles, *Sol. Energy Mater. Sol. Cells*, 2024, **273**, 112955.
2 J. H. Noh, *et al.*, Chemical management for colorful, efficient, and stable inorganic–organic hybrid nanostructured solar cells, *Nano Lett.*, 2013, **13**(4), 1764–1769.
3 Y. Taneja, D. Dube and R. Singh, Recent advances in elemental doping and simulation techniques: improving structural, photophysical and electronic properties of titanium oxide, *J. Mater. Chem. C*, 2024, **12**, 14774–14808.
4 R. Singh and V. K. Shukla, ITIC-based bulk heterojunction perovskite film boosting the power conversion efficiency and stability of the perovskite solar cell, *Sol. Energy*, 2019, **178**, 90–97.
5 R. Singh, S. Sandhu and J.-J. Lee, Elucidating the effect of shunt losses on the performance of mesoporous perovskite solar cells, *Sol. Energy*, 2019, **193**, 956–961.
6 S. Preet and S. T. Smith, A comprehensive review on the recycling technology of silicon based photovoltaic solar panels: Challenges and future outlook, *J. Cleaner Prod.*, 2024, 141661.
7 S. Masi, *et al.*, Connecting the solution chemistry of PbI 2 and MAI: a cyclodextrin-based supramolecular approach to the formation of hybrid halide perovskites, *Chem. Sci.*, 2018, **9**(12), 3200–3208.
8 Z. N. Ndalloka, *et al.*, Solar photovoltaic recycling strategies, *Sol. Energy*, 2024, **270**, 112379.
9 D. Le Khac, *et al.*, Efficient laboratory perovskite solar cell recycling with a one-step chemical treatment and recovery of ITO-coated glass substrates, *Sol. Energy*, 2024, **267**, 112214.
10 F. Deng, *et al.*, Facile eco-friendly process for upcycled sustainable perovskite solar cells, *Chem. Eng. J.*, 2024, **489**, 151228.
11 X. Lyu, *et al.*, Recycling of perovskite solar cells, *Joule*, 2026, **10**(1), 102221.
12 J. Gong, S. B. Darling and F. You, Perovskite photovoltaics: life-cycle assessment of energy and environmental impacts, *Energy Environ. Sci.*, 2015, **8**(7), 1953–1968.
13 J. Zhang, *et al.*, Life cycle assessment of titania perovskite solar cell technology for sustainable design and manufacturing, *ChemSusChem*, 2015, **8**(22), 3882–3891.
14 X.-L. Li, *et al.*, Green solution-processed tin-based perovskite films for lead-free planar photovoltaic devices, *ACS Appl. Mater. Interfaces*, 2018, **11**(3), 3053–3060.
15 A. R. Kadam, H. C. Swart and S. J. Dhoble, Recent Advances in Perovskite Solar Cells, *Mater. Sci. Future Applications*, 2025, 148–158.
16 C. Yang, *et al.*, Achievements, challenges, and future prospects for industrialization of perovskite solar cells, *Light: Sci. Appl.*, 2024, **13**(1), 227.
17 K. Valadez-Villalobos and M. L. Davies, Remanufacturing of perovskite solar cells, *RSC Sustain.*, 2024, **2**(8), 2057–2068.
18 Q. Li, *et al.*, Vertical perovskite solar cell envelope for the circular economy: a case study using life cycle cost analysis in Europe, *J. Cleaner Prod.*, 2024, **467**, 143017.
19 F.-W. Liu, *et al.*, Recycling and recovery of perovskite solar cells, *Mater. Today*, 2021, **43**, 185–197.
20 F. Meng, *et al.*, Recycling Useful Materials of Perovskite Solar Cells toward Sustainable Development, *Adv. Sustainable Syst.*, 2023, **7**(5), 2300014.
21 M. Grätzel, The light and shade of perovskite solar cells, *Nat. Mater.*, 2014, **13**(9), 838–842.
22 A. Wang, *et al.*, Recent promise of lead-free halide perovskites in optoelectronic applications, *Chem. Eng. J.*, 2023, **451**, 138926.
23 J. Jiao, *et al.*, Solvent engineering for the formation of high-quality perovskite films: a review, *Res. Eng.*, 2023, **18**, 101158.
24 S. Y. Park, *et al.*, Sustainable lead management in halide perovskite solar cells, *Nat Sustainability*, 2020, **3**(12), 1044–1051.
25 V. Larini, *et al.*, Sustainable and circular management of perovskite solar cells *via* green recycling of electron transport layer-coated transparent conductive oxide, *Adv. Funct. Mater.*, 2024, **34**(50), 2306040.
26 P. Gunasekara, *et al.*, Water-Based Recycling Process of FTO/SnO_2 Substrate for Sustainable Perovskite Solar Cell Technology, *ChemSusChem*, 2024, **17**(20), e202400939.
27 B. J. Kim, *et al.*, Selective dissolution of halide perovskites as a step towards recycling solar cells, *Nat. Commun.*, 2016, **7**(1), 11735.
28 J. M. Kadro, *et al.*, Proof-of-concept for facile perovskite solar cell recycling, *Energy Environ. Sci.*, 2016, **9**(10), 3172–3179.
29 X. Feng, *et al.*, Close-loop recycling of perovskite solar cells through dissolution-recrystallization of perovskite by butylamine, *Cell Rep. Phys. Sci.*, 2021, **2**(2), 100341.
30 V. Larini, *et al.*, Sustainable decommissioning of perovskite solar cells: from waste to resources, *Chem. Soc. Rev.*, 2025, **54**(15), 7252–7270.
31 M.-G. Ju, *et al.*, Toward eco-friendly and stable perovskite materials for photovoltaics, *Joule*, 2018, **2**(7), 1231–1241.

32 S. Zhang, *et al.*, Cyclic utilization of lead in carbon-based perovskite solar cells, *ACS Sustain. Chem. Eng.*, 2018, **6**(6), 7558–7564.
33 L. Nakka, *et al.*, Analytical review of spiro-OMeTAD hole transport materials: paths toward stable and efficient perovskite solar cells, *Adv. Energy Sustainability Res.*, 2022, **3**(8), 2200045.
34 Y. Li, *et al.*, Gold Nanocrystals and Conjugated Polymer-Wrapped Single-Walled Carbon Nanotube Composites for Catalyzing CO_2 Electroreduction, *ACS Appl. Nano Mater.*, 2025, **8**(17), 9077–9089.
35 S. Krishnamurthy, *et al.*, Yucca-derived synthesis of gold nanomaterial and their catalytic potential, *Nanoscale Res. Lett.*, 2014, **9**, 1–9.
36 R. Singh, *et al.*, Mixed Solvent Engineering to Optimize Morphology and Optical Properties of Perovskite Thin Films for an Efficient Solar Cell, in *The Physics of Semiconductor Devices: Proceedings of IWPSD 2017*, Springer, 2019.
37 R. Singh, *et al.*, Stable triple-cation (Cs+–MA+–FA+) perovskite powder formation under ambient conditions for hysteresis-free high-efficiency solar cells, *ACS Appl. Mater. Interfaces*, 2019, **11**(33), 29941–29949.
38 P. Basumatary and P. Agarwal, Photocurrent transient measurements in MAPbI 3 thin films, *J. Mater. Sci.: Mater. Electron.*, 2020, **31**, 10047–10054.
39 S. Luo, *et al.*, Synthesis and application of non-agglomerated ITO nanocrystals *via* pyrolysis of indium–tin stearate without using additional organic solvents, *J. Nanopart. Res.*, 2014, **16**, 1–12.
40 Z. S. Almutawah, *et al.*, Enhanced grain size and crystallinity in CH_3 NH_3 PbI_3 perovskite films by metal additives to the single-step solution fabrication process, *MRS Adv.*, 2018, **3**, 3237–3242.
41 S. Arya, *et al.*, Electrochemical detection of ammonia solution using tin oxide nanoparticles synthesized *via* sol–gel route, *Appl. Phys.*, 2018, **124**, 1–7.
42 H. Nayak, *et al.*, Performance of SnO_2 Thin Film Prepared by CWD Technique on Different Substrates for Device Applications: An Innovative Approach, *J. Electron. Mater.*, 2024, **53**(8), 4645–4660.
43 M. Kundar, *et al.*, Stable Perovskite Solar Cells Based on Direct Surface Passivation Employing 2D Perovskites, *Sol. RRL*, 2023, **7**(23), 2300572.
44 R. Singh and M. Parashar, Origin of hysteresis in perovskite solar cells, *Soft-Matter Thin Film Sol. Cells*, 2020, **12**, 30.
45 S. K. Yadavalli, *et al.*, Electron-beam-induced cracking in organic-inorganic halide perovskite thin films, *Scr. Mater.*, 2020, **187**, 88–92.
46 Z. Dai and N. P. Padture, Challenges and opportunities for the mechanical reliability of metal halide perovskites and photovoltaics, *Nat. Energy*, 2023, **8**(12), 1319–1327.
47 F. Zhou, *et al.*, Synthesis of polyethylenes with in-chain isolated carbonyls from CO_2 and ethylene *via* a tandem photoreduction/polymerization protocol, *CCS Chem.*, 2024, **6**(6), 1591–1599.
48 P. Kumar, S. K. Sharma and R. Singh, A hydrophobic organic spacer cation for improving moisture resistance and efficiency in mixed-dimensional perovskite solar cells, *EES Solar*, 2025, **1**(3), 356–365.
49 M. Kundar, *et al.*, Surface passivation by sulfur-based 2D (TEA) $2PbI_4$ for stable and efficient perovskite solar cells, *ACS Omega*, 2023, **8**(14), 12842–12852.
50 S. Akel, *et al.*, Charge Carrier Collection Losses in Lead-Halide Perovskite Solar Cells, *Adv. Energy Mater.*, 2024, 2401800.
51 C. M. Alder, *et al.*, Updating and further expanding GSK's solvent sustainability guide, *Green Chem.*, 2016, **18**(13), 3879–3890.
52 A. Binek, *et al.*, Recycling perovskite solar cells to avoid lead waste, *ACS Appl. Mater. Interfaces*, 2016, **8**(20), 12881–12886.
53 B. Augustine, *et al.*, Recycling perovskite solar cells through inexpensive quality recovery and reuse of patterned indium tin oxide and substrates from expired devices by single solvent treatment, *Sol. Energy Mater. Sol. Cells*, 2019, **194**, 74–82.